Gas-filled ultrasound microbubbles enhance the immunoactivity of the HSP70-MAGEA1 fusion protein against MAGEA1-expressing tumours

XING GAO[1*], YANG NAN[2*], YUAN YUAN[1], XUE GONG[3], YUANYUAN SUN[3], HUIHUI ZHOU[3], YUJIN ZONG[4], LIJUN ZHANG[5] and MING YU[3]

[1]State Key Laboratory of Cancer Biology and Department of Pathology, Xijing Hospital, The Fourth Military Medical University, Xi'an, Shaanxi 710032; [2]Department of Gynecology, The First Affiliated Hospital of Xi'an Medical University, Xi'an, Shaanxi 710077; [3]Department of Ultrasound, Xijing Hospital, The Fourth Military Medical University, Xi'an, Shaanxi 710032; [4]Key Laboratory of Biomedical Information Engineering of Ministry of Education, Department of Biomedical Engineering, School of Life Science and Technology, Xi'an Jiaotong University, Xi'an, Shaanxi 710049; [5]Department of Clinical Diagnosis, Tangdu Hospital, The Fourth Military Medical University, Xi'an, Shaanxi 710038, P.R. China

Received September 25, 2017; Accepted April 16, 2018

DOI: 10.3892/mmr.2018.9003

Abstract. Advanced malignant melanoma is characterized by rapid development, poor prognosis and insensitivity to chemoradiotherapy. Immunotherapy has become one of the primary clinical treatments for malignant melanomas. In recent decades, identifying specific tumour antigens and the enhanced immunoactivity of tumour vaccines has become critical for engineering successful tumour vaccines. As a widely used vaccine carrier, heat shock protein 70 (HSP70) clearly increases the immunogenicity of tumour antigens, such as melanoma-associated antigen A1 (MAGEA1). Based on previous studies, gas-filled ultrasound microbubbles (MBs) were engineered to carry an HSP70-MAGEA1 fusion protein (FP). Following subcutaneous injection around the lymphatic nodes the FP was directly released into the lymph nodes under ultrasonic imaging. The results indicated that the microbubbles enhanced the immunoactivity of FPs more effectively than HSP70-MAGEA1 fusion alone. Additionally, HSP70-MAGEA1 delivered via microbubbles clearly inhibited and delayed the growth of MAGEA1-expressing B16 melanomas in mice and improved the survival times of these animals compared with the fusion protein alone. The results of the present study demonstrated that controlled MBs enhance the immunoactivity of FPs and also highlights novel, potential vaccine carriers and a new strategy for engineering controllable tumour vaccine designs.

Correspondence to: Dr Ming Yu, Department of Ultrasound, Xijing Hospital, The Fourth Military Medical University, 15 Changle West Road, Xi'an, Shaanxi 710032, P.R. China
E-mail: yumingfmmu@126.com

*Contributed equally

Abbreviations: HSP70, heat shock protein 70; MAGEA1, melanoma-associated antigen A1; MB, gas-filled ultrasound microbubbles; FP, HSP70-MAGEA1 fusion protein; MB-FP, gas-filled ultrasound microbubbles with HSP70-MAGEA1 fusion protein

Key words: gas-filled ultrasound microbubbles, heat shock protein 70-melanoma-associated antigen A1 fusion protein, tumour vaccine

Introduction

Tumour vaccines have become the hot spots of anticancer immunotherapy in recent decades, and tumour-specific antigens (TSAs) have been used to induce specific cellular and humoural immune responses to inhibit tumour occurrence and development. TSAs can stimulate specific immune responses and are the main components in tumour vaccines. As the first discovered TSA, Melanoma-associated antigen A1 (MAGEA1) is expressed in most tumours, including the testes and placenta (1-3). MAGEA1 be processed and presented by human leukocyte antigen (HLA) class I molecules on cancer cells, and MAGEA1-expressing cancer cells can be rejected by host cytotoxic T lymphocytes (CTLs) (4,5). Tumour vaccines based on MAGEA1 have been used in patients with a variety of tumours, but most of these vaccines do not exhibit particularly significant clinical effects on cancer (6-10). Therefore, it is imperative to explore more effective TSA-based tumour vaccines.

As a molecular chaperone, heat shock protein 70 (HSP70) participates in processing and presenting tumour antigens, and HSP70 fused with TSA can significantly enhance cellular and humoural immune responses against cancer cells (11). Moreover, previous studies have shown that the HSP70-MAGEA1 fusion protein can stimulate MAGEA1-specific antitumour immunity (11-13). However,

the immunoactivity of HSP70 fusion proteins needs further improvement for their clinical application. In recent years, gas-filled microbubbles (MBs) have been used in the clinic as intravenously administered ultrasound-based contrast agents (14,15) due to their high acoustic impedance mismatch between gases and blood (16,17). The delivery of DNA/RNA/protein in target cells by the application of ultrasound, a process known as sonoporation, has successfully been applied (18,19) and demonstrated as a good candidate for lipid-based TSA delivery. Gas-filled ultrasound microbubbles can transport drugs or genes across cell membranes and vessel walls and are considered effective transport carriers *in vivo*. Moreover, gas-filled ultrasound microbubbles are efficiently phagocytosed and presented bydendritic cells (DC) and activate stronger immune responses (20,21).

In the present study, we used gas-filled ultrasound microbubbles as carriers for the controllable release of HSP70-MAGEA1 fusion proteins at a specific location and evaluated the immunoactivity of antitumours to explore a new strategy for future tumour immunotherapy.

Materials and methods

Animals and cell lines. C57BL/6 mice (8 weeks old) were provided from the Laboratory Animal Center of the Fourth Military Medical University and fed in a specific pathogen-free (SPF) animal house. All experiments were conducted according to the guidelines for the Care and Use of Laboratory Animals and approved by the Animal Ethical Committee of the Fourth Military Medical University. B16 cell lines overexpressing MAGEA1 (B16-MAGEA1) were previously established (22).

Preparation and identification of gas-filled ultrasound microbubbles (MBs). The MBs were prepared as previously reported (23). Briefly, a mixture of the nonionic surfactant Span 60 (3 wt%), Tween 80 (5 wt%), and polyethylene glycol (PEG; 3 wt%) with different polymerization degrees were sonicated in PBS solution using a high-intensity ultrasonic processor (VCX-750; Sonix, USA) for 1 min at 400 W in the presence of sulfur hexafluoride (SF_6) gas. Then, the mixture was incubated in a separating funnel for 30 min, and the middle layer, comprising the microbubbles, was separated and washed with PBS. To prepare the fusion protein-loaded microbubbles (MB-FP), 200 μl of HSP70-MAGEA1 was incubated with 1 ml of MBs for 10 min at 4˚C, and the fusion proteins were adsorbed onto the MBs via electrostatic adsorption self-assembly. Unloaded protein was removed after three centrifugal washes with PBS buffer solution. After washing, the size distribution of the protein-loaded microbubbles was measured using a Coulter counter (Multisizer III, Beckman-Coulter, Pasadena, CA, USA) (15). After extraction, the protein concentration was measured using the Bradford method. The prepared gas-filled ultrasound microbubbles were stored in sealed glass vials under a headspace filled with SF_6 gas at 4˚C.

Immunization regime. C57BL/6 mice were subcutaneously (s.c.) immunized in the foreleg with 10 μg/100 μl/mouse gas-filled ultrasound microbubbles carrying HSP70-MAGEA1 fusion protein (MB-FP group), and HSP70-MAGEA1 fusion protein alone (FP group) or gas-filled ultrasound microbubbles (MB group) alone were used as controls. After administration, the MBs were destroyed near the inguinal lymph nodes with a mechanical index (MI=0.7). Three administrations at one-week intervals were performed, and the sera and spleen were collected for experiments at two weeks after the last injection.

Immunoblotting analysis. The lymph nodes from vaccinated mice were used for immunoblotting to detect HSP70 and MAGEA1 proteins. The total proteins were extracted from the spleens using RIPA buffer, and the cell debris was removed by centrifugation at 12,000 x g for 20 min at 4˚C. After quantification, 10-50 μg/lane of the spleen proteins were separated by SDS-PAGE. The MAGEA1 and HSP70 proteins were detected using anti-human MAGEA1 and anti-HSP70 (both Abcam, Cambridge, UK) antibodies, respectively.

IFNγ enzyme-linked immunosorbent spot (ELISpot) assay. The mouse IFNγ ELISpot assay was performed as previously described (22) in PVDF-bottomed 96-well plates (Millipore, USA) using a commercial kit (Diaclone, France). Briefly, the plates were covered with an anti-IFNγ antibody overnight at 4˚C and blocked with 5% non-fat skimmed milk. The splenocytes ($2x10^5$ cells/well) were then inoculated together with the indicated number of lethally irradiated B16-MAGEA1 cells ($2x10^4$/well, respectively). After incubation for 24 h, the cells were removed, and a biotinylated IFNγ detection antibody was added for 2 h and incubated with streptavidin-alkaline phosphatase for another 1 h at 37˚C. After washing with PBST, the spots were visualized by the addition of the alkaline phosphatase substrate BCIP/NBT and counted using a dissection microscope. The number of MAGEA1-specific T-cell precursors in the splenocytes was calculated by subtracting the IFNγ+ spots of splenocytes on B16-stimulating cells from that on B16-MAGEA1 cells.

ELISA. Irradiated B16-MAGEA1 cells ($5x10^5$) were cocultured with splenocytes ($5x10^6$ cells) from mice at 2 weeks after the last vaccination, and the cells were cultured in 2 ml of DMEM supplemented with 10% foetal bovine serum (FBS), 2 mM L-glutamine, 100 U/ml penicillin and 100 μg/ml streptomycin in 24-well tissue culture plates for 72 h. Murine IL-2 ELSIA kits (Diaclonek, France) were used to assay the presence of IL-2 in the supernatants according to the manufacturer's instructions. The titre of anti-MAGEA1 antibody in the sera was determined as previously described (22).

Tumour treatmente. The mice were s.c. challenged with B16-MAGEA1 tumour cells ($1x10^6$ cells/mouse, respectively) in the hind legs (D0) as previously described (22). One week later (day 7), the mice were s.c. vaccinated with 10 μg/100 μl/mouse MB-FP (gas-filled ultrasound microbubbles with HSP70-MAGEA1 fusion protein) in the forelegs. The control groups were s.c. injected with 10 μg/100 μl/mouse HSP70-MAGEA1 fusion protein alone or gas-filled microbubbles alone. Every group included 10 mice. At one week (day 14) and 2 weeks (day 21) later, these mice were boosted with the same regimes. The tumour volumes (length x $width^2$x $\pi/6$) and weight were measured twice a week after the tumours became palpable and were plotted as the mean tumour volume of the

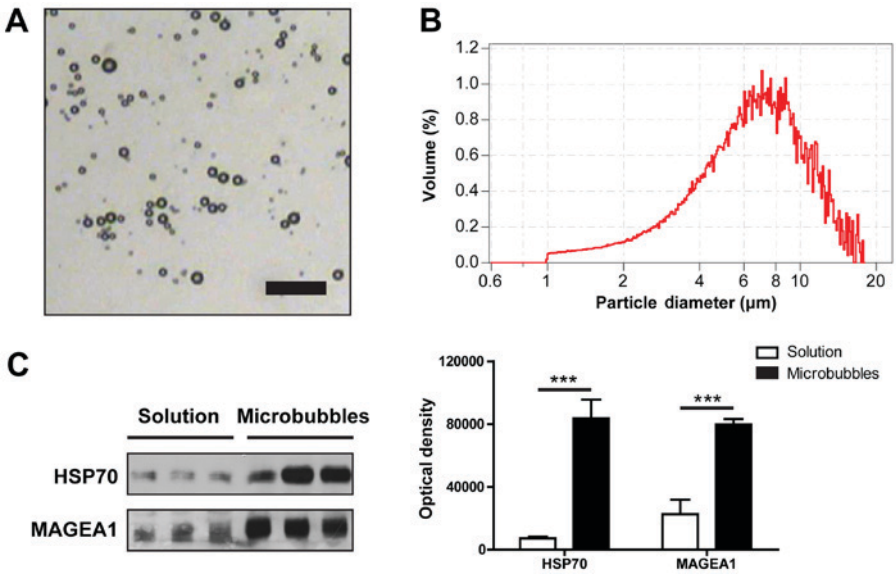

Figure 1. The generation of MB-FP. (A) Representative photo of gas-filled microbubbles carrying the HSP70-MAGEA1 fusion protein. Scale bar, 50 μm. (B) Size distribution curve of MB-FP. (C) Western blots and densitometric analysis of HSP70 and MAGEA1 protein levels in solution and microbubble fractions. Data are the mean ± SEM (n=3). Two-way analysis of variance with Bonferroni post-test, ***P<0.001 vs. the optical density of the solution group. HSP70, heat shock protein 70; MAGEA1, melanoma-associated antigen A1; MB-FP, gas-filled ultrasound microbubbles with HSP70-MAGEA1 fusion protein.

group (means ± SEM) vs. the number of days after the tumour was planted. The survival time of the mice was also recorded.

Tumour challenge experiments. The mice were vaccinated (day 21) with MB-FP, HSP70-MAGEA1 fusion protein or gas-filled microbubbles (10 mice per group), as previously described (12,13). At one week (day 14) and 2 weeks later (day 7), the immunization regime was boosted twice. On the 7th day after the last immunization (day 0), the mice were s.c. challenged with B16-MAGEA1 tumour cells ($1x10^5$ cells/mouse, respectively) in the hind legs. Once the tumours became palpable, observations were taken twice a week, and the ratio of tumour-free mice was recorded.

Statistical analysis. All statistical analyses were carried out using Graphpad Prism 5 software (GraphPad, USA). Results are presented as the means ± SEM. Data were analyzed by one-way analysis of variance (ANOVA) with Tukey's Multiple Comparison test and two-way ANOVA with Bonferroni post-test. Kaplan-Meier survival plots and the log-rank test were used to evaluate differences in animal survival among experimental groups (P-value).

Results

Gas-filled microbubbles effectively delivered HSP70-MAGE-A1 fusion proteins to subcutaneous lymph nodes. The gas-filled ultrasound microbubbles (MBs) were generated as described in the Methods, and a representative microscopic picture of the MBs is shown in Fig. 1A. The mean diameter of the microbubbles was 6.02 μm, and approximately 90% microbubbles were smaller than 13.86 μm in diameter (Fig. 1B). Through electrostatic attraction, HSP70-MAGEA1 fusion proteins were easily adsorbed onto the shells of these MBs. Immunoblotting and densitometric analysis indicated that the vast majority of MBs were combined with the HSP70-MAGEA1 fusion protein (Fig. 1C). The concentration of MBs was approximately $3.2x10^8$/ml, and the protein concentration was approximately 100 μg/ml. Prior to injection, the sample was further diluted with PBS solution (pH=7.4).

As microbubbles are primarily used as ultrasonic contrast agents, we therefore followed the kinetics of MBs persistence *in vivo* after s.c. injection in the forelegs. Under contrast-enhanced ultrasound-mediated visualization of the low mechanical index ultrasound pulse signal persistence, the MBs were clearly detected in the lymph nodes (Fig. 2A). After destroying the MBs with a mechanical index (MI=0.75), the lymph nodes were dissected and the levels of HSP70-MAGEA1 fusion proteins were analysed. The immunoblotting and densitometric results indicated that both HSP70 and MAGEA1 proteins could be detected after immunization. However, the antigens to MAGEA1 were higher in the lymph nodes of mice immunized with MB-FP than in those immunized with FP alone (Fig. 2B). These results showed that gas-filled ultrasound microbubbles could improve the delivery of HSP70-MAGEA1 antigen to the lymph tissues.

Gas-filled microbubbles could boost the specific immune responses against MAGEA1. CTLs are one of the most important antitumour effectors of the cell immune response *in vivo*. To determine whether MBs enhanced the cellular immune response, the IFN-γ ELISpot assay was used to determine the number of MAGEA1-specific $CD8^+$ T cells in the splenocytes from mice immunized with gas-filled ultrasound microbubbles (MB), HSP70-MAGEA1 fusion protein (FP) alone and gas-filled ultrasound microbubbles carrying the HSP70-MAGEA1 fusion protein (MB-FP). The results showed that the number of spot-forming T-cell precursors specific to MAGEA1-expressing B16 cells were significantly higher in the splenocytes of mice vaccinated with MB-FP compared with that in mice vaccinated with FP or MB alone (Fig. 3A). These results suggested that

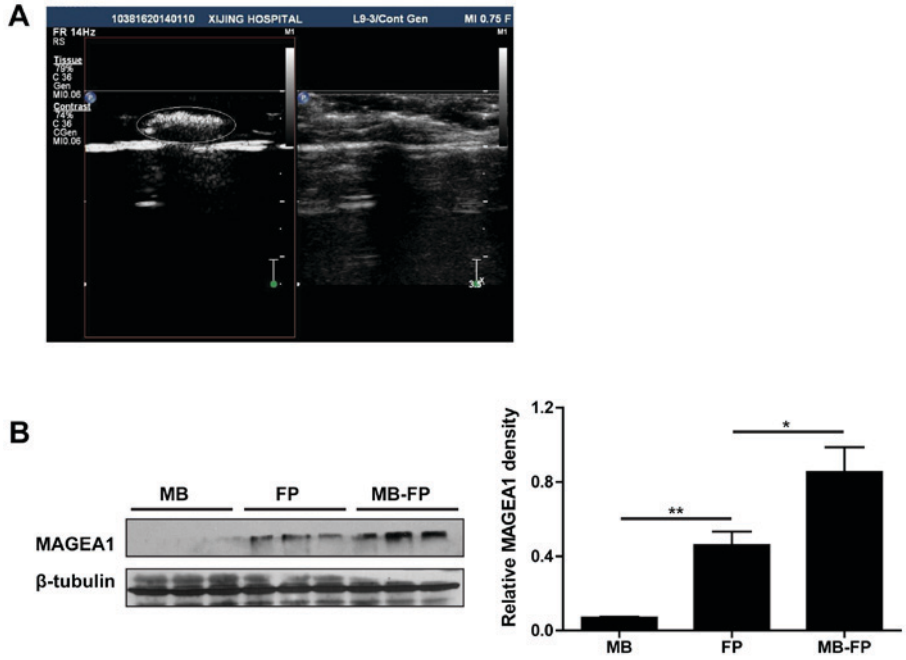

Figure 2. The visualization and targeted release of gas-filled microbubbles with HSP70-MAGEA1 fusion protein (MB-FP). (A) The representative images of MB-FP *in vivo* under ultrasound (Left), and representative images of MB-FP destroyed using a mechanical index (MI=0.75) (Right). (B) Immunoblotting and densitometric analysis of MAGEA1 in lymph nodes from mice using different methods of immunization. Data are the mean ± SEM (n=3). One-way analysis of variance with Tukey's Multiple Comparison test, *P<0.05 and **P<0.01. MB, gas-filled ultrasound microbubbles; FP, HSP70-MAGEA1 fusion protein; MB-FP, gas-filled microbubbles with HSP70-MAGEA1 fusion protein; HSP70, heat shock protein 70; MAGEA1, melanoma-associated antigen A1.

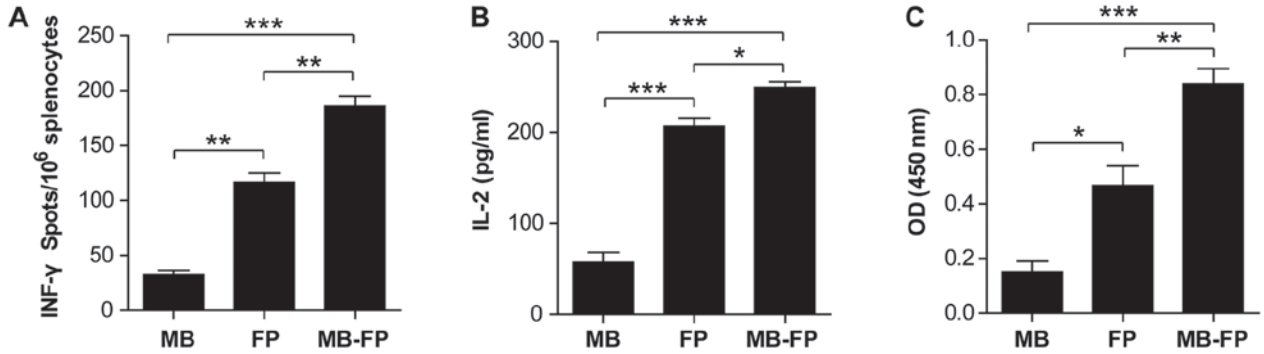

Figure 3. The cellular and humoural immune responses of gas-filled microbubbles with HSP70-MAGEA1 fusion proteins. (A) IFNγ ELISpot assays of MAGEA1-specific T-cell precursors from the splenocytes of mice vaccinated with MB, FP, and gas-filled microbubbles with MB-FP (n=10). (B) The levels of IL-2 secretions from splenocytes of vaccinated mice were measured using ELISA (n=10). (C) The anti-MAGEA1 antibody titres in the sera of vaccinated mice (n=10). The data are presented as the means ± SEM and analysed by one-way analysis of variance with Tukey's Multiple Comparison Test. *P<0.05, **P<0.01 and ***P<0.001. HSP70, heat shock protein 70; MAGEA1, melanoma-associated antigen A1; MB, gas-filled ultrasound microbubbles; FP, HSP70-MAGEA1 fusion protein; MB-FP, gas-filled ultrasound microbubbles with HSP70-MAGEA1 fusion protein; IFN, interferon.

MBs could significantly enhance specific immune responses, although HSP70-MAGEA1 fusion proteins alone also stimulated the generation of INFγ-producing MAGEA1-specific T-cell precursors *in vivo*. We then analysed the IL-2 secretion of splenocytes in mice treated with various vaccines using ELISA to further determine the T-cell-mediated antitumour immune responses. As shown in Fig. 3B, the IL-2 levels in the supernatant of cocultured irradiated B16-MAGEA1 and splenocytes from mice vaccinated with MB-FP were significantly higher than in the cells from mice vaccinated with FP or MB alone. Combined with the data from ELISpot assay, these results suggested that the gas-filled microbubbles enhanced the generation of MAGEA1-specific cellular immune responses by HSP70-MAGEA1 fusion proteins.

To evaluate the humoural immune responses, the titres of anti-MAGEA1 antibody in the sera of the vaccinated mice were determined using ELISA after the last vaccination. As shown in Fig. 3C, the levels of anti-MAGEA1 antibody were significantly boosted in the mice vaccinated with FP or MB-FP, and the titres of anti-MAGEA1 were slightly higher in mice vaccinated with MB-FP compared with those in mice vaccinated with FP alone. These results indicated that the MB-FP could elicit and boost MAGEA1-specific humoural immune responses (Fig. 3B). Collectively, these results verified that HSP70-MAGEA1 fusion proteins delivered via gas-filled ultrasound microbubbles could more effectively boost both cellular and humoural immune responses against MAGEA1 compared with the fusion protein alone.

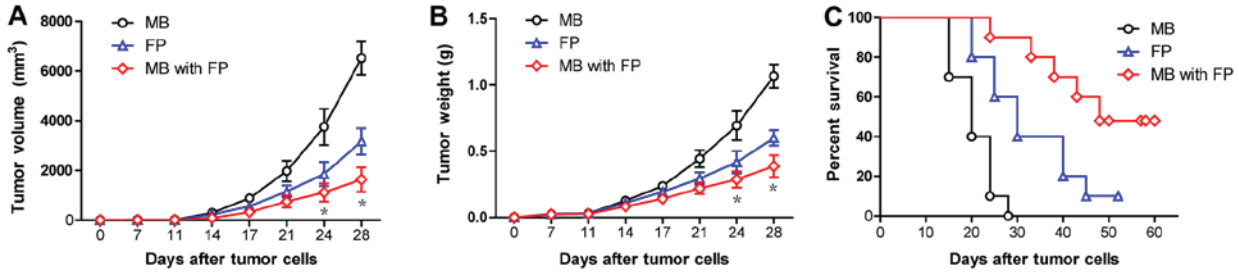

Figure 4. The immunotherapy of pre-established B16-MAGEA1 melanoma with gas-filled microbubbles with HSP70-MAGEA1 fusion protein. The mice were s.c. inoculated with MAGEA1-expressing B16 (B16-MAGE-A1) cells (10^6 cells/mouse) on day 0 and were then administered MB, FP, and MB-FP on days 7, 14 and 21. (A and B) Vaccination with MB-FP significantly delayed the tumour growth of B16-MAGEA1 compared with vaccination with FP and MB (n=10). *P<0.05 vs. the FP group. Two-way ANOVA with Bonferroni post-test. (C) MB-FP vaccination could significantly increase the survival time compared with FP or MB alone in B16-MAGEA1 tumour-bearing mice (n=10). Log-rank test, FP vs. MB, P=0.0011; MB with FP vs. MB, P<0.001; MB with FP vs. FP, P=0.0295. HSP70, heat shock protein 70; MAGEA1, melanoma-associated antigen A1; MB, gas-filled ultrasound microbubbles; FP, HSP70-MAGEA1 fusion protein; MB-FP, gas-filled ultrasound microbubbles with HSP70-MAGEA1 fusion protein.

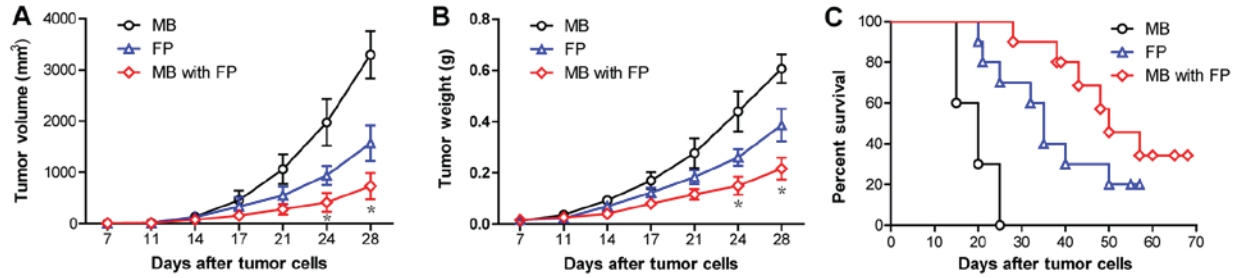

Figure 5. The preventive effects of gas-filled microbubbles with HSP70-MAGEA1 fusion protein on B16-MAGEA1 melanoma. The mice were vaccinated with MB-FP, MB and FP as described in the Materials and methods and then challenged with $1x10^6$ B16-MAGEA1 melanoma cells (n=10). (A and B) The MB-FP vaccination slowed the tumour volumes of B16-MAGEA1 cells. *P<0.05 vs. the FP group. Two-way ANOVA with Bonferroni post-hoc test. (C) MB-FP prolonged the survival times compared with the mice vaccinated with FP and MB (n=10). Log-rank test: FP vs. MB, P=0.0007; MB with FP vs. MB, P<0.001; MB with FP vs. FP, P=0.0459. MB, gas-filled ultrasound microbubbles; FP, HSP70-MAGEA1 fusion protein; MB-FP, gas-filled ultrasound microbubbles with HSP70-MAGEA1 fusion protein; MAGEA1, melanoma-associated antigen A1; HSP70, heat shock protein 70.

HSP70-MAGEA1 fusion protein delivered via gas-filled microbubbles delayed tumour growth and prolonged the survival of mice. To investigate the clinical efficacy of MB-FP and FP vaccines against MAGEA1-expressing tumours, the mice were s.c. inoculated with MAGEA1-expressing B16 (B16-MAGEA1) cells (10^6 cells/mouse) on day 0, and 10 μg/100 μl/mouse of different vaccines was administered on days 7, 14 and 21. The results showed that MB-FP vaccination significantly delayed the growth of B16-MAGEA1 tumours compared with mice vaccinated with FP and MB only (Fig. 4A & B). Moreover, the survival times of mice with pre-existing B16-MAGEA1 tumours were significantly prolonged after vaccinated with MB-FP compared with mice vaccinated with FP and MB only (Fig. 4C). These results suggested that the use of gas-filled microbubbles significantly increases the immunoactivity of HSP70-MAGEA1 fusion proteins and improves the survival of mice bearing melanomas, suggesting that MB-FP is a potent and efficient therapeutic vaccine against MAGEA1-expressing tumours.

HSP70-MAGE-A1 fusion protein delivered via gas-filled microbubbles is an efficient protective vaccine against MAGEA1-expressing tumours. To determine the protective effects of MB-FP vaccines, the mice were vaccinated with MB-FP, MBs and FP as described in the Materials and methods and were then challenged with $1x10^6$ B16-MAGEA1 melanoma cells. The mice were monitored for evidence of tumour growth by palpation and inspection. The results showed that MB-FP vaccination slowed the tumour volumes and weight of B16-MAGEA1 cells (Fig. 5A & B) and prolonged the survival times compared with those in the mice vaccinated with FP and MBs alone (Fig. 5C). In conclusion, these results showed that MB-FP exhibited protective effects against MAGEA1-expressing tumours.

Discussion

As an important member of melanoma antigen, MAGEA1 is expressed in most tumours but not in normal tissues, except testis and ovary. MAGEA1 encodes several antigenic peptides that bind to HLA class I molecules and are recognized by T lymphocytes. To improve the immunoactivity of MAGEA1, several adjuvant molecules have been used. Heat shock protein 70 (HSP70) plays an important role in protein trafficking, folding and antigen presentation. A previous study showed that HSP70 could be exploited to enhance the cellular and humoural immune responses against any attached tumour-specific antigens (TSA) (11). Moreover, the fusion proteins of HSP70 and TSA have been demonstrated to be powerful strategies to increase immunogenicity (24-26). However, a targeted delivery system could effectively increase the immunoactivity and improve the clinical applications of HSP70 fusion proteins.

Recently, gas-filled ultrasound microbubbles (MBs) have been used in the clinic as intravenously administered ultrasound-based contrast agents (16,27-29), as microbubbles oscillate and vibrate when a sonic energy field is applied and may reflect ultrasound waves, distinguishing the microbubbles from surrounding tissues. Moreover, gas-filled microbubbles can be used as protein carriers when the shells of microbubbles are composed of special molecules (23,30,31).

Compared with other carriers, the components of gas-filled microbubbles are biodegradable materials, so these compounds do not exhibit immunogenicity, and gas-filled ultrasound microbubbles are small and relatively stable and can remain stable in the body. Moreover, gas-filled ultrasound microbubbles could be broken under ultrasonic irradiation in a targeted area, achieving targeted drug release (32-34). In addition, the ultrasound-mediated microbubble destruction could also increase cell membrane permeability, thereby increasing the drug concentration in the target cell. These advantages make gas-filled microbubbles ideal delivery carriers (20,35).

Gas-filled microbubbles are used in therapeutic applications based on the intrinsic sonoporation ability of the encapsulated drugs. Microbubbles coupled with ultrasound exposure have been studied for opening the blood-brain barrier (BBB) and delivering drugs (36-38). Combining siRNA silencing ABCG2-loaded mPEG-PLGA-PLL nanoparticles and ultrasound-targeted Microbubbles destruction enhanced therapeutic effect of Adriamycin on multidrug-resistant breast cancer (39). Thrombus-targeting Microbubbles, which have fibrinolytic drugs on the surface reduced the size of the thrombus via ultrasound imaging without prolonging bleeding time (40).

In the present study, we presented a new strategy for the targeted release of HSP70-MAGEA1 fusion proteins. The proposed polymer gas-filled microbubbles were used as targeted delivery carriers of the fusion protein HSP70-MAGEA1 for subcutaneous delivery around superficial lymph nodes. After the contrast agent into the specific lymph nodes, the gas-filled ultrasound microbubbles carrying the HSP70-MAGEA1 fusion protein released the immunizing antigen, which effectively increased the generation of specific antitumour immune responses.

Consistent with the immune responses, the results of tumour treatment and protection *in vivo* demonstrated that gas-filled microbubbles could increase the antitumour effects of HSP70-MAGEA1 fusion proteins. Tumour xenografts in mice from B16-MAGE-A1 cells were immunized with MB-FP grew significantly slower compared with those from mice immunized with the HSP70-MAGEA1 fusion protein alone, and the survival times of the mice were significantly prolonged, demonstrating that gas-filled microbubbles could enhance the therapeutic immunization of HSP70-MAGEA1 fusion protein. Furthermore, we showed that the HSP70-MAGEA1 delivered via gas-filled microbubbles was more proficient at protecting against tumour development when used earlier in the progression of cancer, suggesting the preferential application of this tumour vaccine to prevent tumour recurrence in postoperative cancer patients.

In conclusion, these results showed that the gas-filled microbubble-mediated delivery of HSP70-MAGEA1 fusion protein as a tumour vaccine could be used for targeted release at lymph nodes, thereby effectively improving the antitumour efficacy of the HSP70-MAGEA1 fusion protein. The present study not only described a new strategy for targeted tumour biological treatments using HSP70 fusion proteins but also provided a research basis for controllable drug carriers for clinical application.

Acknowledgements

The present study was financially supported by grants from the National Natural Science Foundation of China (nos. 81670792 and 31671416), and the Booster Programme of Xijing Hospital.

Competing interests

The authors declare that they have no competing interests.

References

1. Fang JB and Wang L: The function of tumor specific antigen (MAGE) in tumor immunotherapy. Sheng Li Ke Xue Jin Zhan 36: 273-275, 2005 (In Chinese).
2. Xiao J and Chen HS: Biological functions of melanoma-associated antigens. World J Gastroenterol 10: 1849-1853, 2004.
3. Xiao J and Chen HS: Biological functions of melanoma-associated antigens (MAGEs) in cell activities. Ai Zheng 24: 124-128, 2005 (In Chinese).
4. Sudo T, Kuramoto T, Komiya S, Inoue A and Itoh K: Expression of MAGE genes in osteosarcoma. J Orthop Res 15: 128-132, 1997.
5. van der Bruggen P, Traversari C, Chomez P, Lurquin C, De Plaen E, Van den Eynde BJ, Knuth A and Boon T: A gene encoding an antigen recognized by cytolytic T lymphocytes on a human melanoma. J Immunol 178: 2617-2621, 2007.
6. van Baren N, Bonnet MC, Dréno B, Khammari A, Dorval T, Piperno-Neumann S, Liénard D, Speiser D, Marchand M, Brichard VG, *et al*: Tumoral and immunologic response after vaccination of melanoma patients with an ALVAC virus encoding MAGE antigens recognized by T cells. J Clin Oncol 23: 9008-9021, 2005.
7. Slingluff CL Jr, Petroni GR, Olson W, Czarkowski A, Grosh WW, Smolkin M, Chianese-Bullock KA, Neese PY, Deacon DH, Nail C, *et al*: Helper T-cell responses and clinical activity of a melanoma vaccine with multiple peptides from MAGE and melanocytic differentiation antigens. J Clin Oncol 26: 4973-4980, 2008.
8. Mackensen A, Herbst B, Chen JL, Köhler G, Noppen C, Herr W, Spagnoli GC, Cerundolo V and Lindemann A: Phase I study in melanoma patients of a vaccine with peptide-pulsed dendritic cells generated in vitro from CD34(+) hematopoietic progenitor cells. Int J Cancer 86: 385-392, 2000.
9. Chianese-Bullock KA, Pressley J, Garbee C, Hibbitts S, Murphy C, Yamshchikov G, Petroni GR, Bissonette EA, Neese PY, Grosh WW, *et al*: MAGE-A1-, MAGE-A10-, and gp100-derived peptides are immunogenic when combined with granulocyte-macrophage colony-stimulating factor and montanide ISA-51 adjuvant and administered as part of a multipeptide vaccine for melanoma. J Immunol 174: 3080-3086, 2005.
10. Akiyama Y, Tanosaki R, Inoue N, Shimada M, Hotate Y, Yamamoto A, Yamazaki N, Kawashima I, Nukaya I, Takesako K, *et al*: Clinical response in Japanese metastatic melanoma patients treated with peptide cocktail-pulsed dendritic cells. J Transl Med 3: 4, 2005.
11. Ge W, Sui YF, Wu DC, Sun YJ, Chen GS, Li ZS, Si SY, Hu PZ, Huang Y and Zhang XM: MAGE-1/Heat shock protein 70/MAGE-3 fusion protein vaccine in nanoemulsion enhances cellular and humoral immune responses to MAGE-1 or MAGE-3 in vivo. Cancer Immunol Immunother 55: 841-849, 2006.
12. Ge W, Li Y, Li ZS, Zhang SH, Sun YJ, Hu PZ, Wang XM, Huang Y, Si SY, Zhang XM and Sui YF: The antitumor immune responses induced by nanoemulsion-encapsulated MAGE1-HSP70/SEA complex protein vaccine following peroral administration route. Cancer Immunol Immunother 58: 201-208, 2009.

13. Ge W, Hu PZ, Huang Y, Wang XM, Zhang XM, Sun YJ, Li ZS, Si SY and Sui YF: The antitumor immune responses induced by nanoemulsion-encapsulated MAGE1-HSP70/SEA complex protein vaccine following different administration routes. Oncol Rep 22: 915-920, 2009.
14. Gkegkes ID and Iavazzo C: Contrast Enhanced Ultrasound (CEU) using microbubbles for sentinel lymph node biopsy in breast cancer: A systematic review. Acta Chir Belg 115: 212-218, 2015.
15. Stride E: Physical principles of microbubbles for ultrasound imaging and therapy. Front Neurol Neurosci 36: 11-22, 2015.
16. Wilson SR and Burns PN: Microbubble-enhanced US in body imaging: What role? Radiology 257: 24-39, 2010.
17. Wan C, Li F and Li H: Gene therapy for ocular diseases meditated by ultrasound and microbubbles (Review). Mol Med Rep 12: 4803-4814, 2015.
18. Suzuki R, Oda Y, Utoguchi N, Namai E, Taira Y, Okada N, Kadowaki N, Kodama T, Tachibana K and Maruyama K: A novel strategy utilizing ultrasound for antigen delivery in dendritic cell-based cancer immunotherapy. J Control Release 133: 198-205, 2009.
19. Lemmon JC, McFarland RJ, Rybicka JM, Balce DR, McKeown KR, Krohn RM, Matsunaga TO and Yates RM: In vitro and in vivo transfection of primary phagocytes via microbubble-mediated intraphagosomal sonoporation. J Immunol Methods 371: 152-158, 2011.
20. Bioley G, Lassus A, Bussat P, Terrettaz J, Tranquart F and Corthésy B: Gas-filled microbubble-mediated delivery of antigen and the induction of immune responses. Biomaterials 33: 5935-5946, 2012.
21. Bioley G, Bussat P, Lassus A, Schneider M, Terrettaz J and Corthésy B: The phagocytosis of gas-filled microbubbles by human and murine antigen-presenting cells. Biomaterials 33: 333-342, 2012.
22. Ye J, Chen GS, Song HP, Li ZS, Huang YY, Qu P, Sun YJ, Zhang XM and Sui YF: Heat shock protein 70/MAGE-1 tumor vaccine can enhance the potency of MAGE-1-specific cellular immune responses in vivo. Cancer Immunol Immunother 53: 825-834, 2004.
23. Li S, Zhu C, Fang S, Zhang W, He N, Xu W, Kong R and Shang X: Ultrasound microbubbles enhance human β-defensin 3 against biofilms. J Surg Res 199: 458-469, 2015.
24. Ma JH, Sui YF, Ye J, Huang YY, Li ZS, Chen GS, Qu P, Song HP and Zhang XM: Heat shock protein 70/MAGE-3 fusion protein vaccine can enhance cellular and humoral immune responses to MAGE-3 in vivo. Cancer Immunol Immunother 54: 907-914, 2005.
25. Suzue K and Young RA: Adjuvant-free hsp70 fusion protein system elicits humoral and cellular immune responses to HIV-1 p24. J Immunol 156: 873-879, 1996.
26. Mizukami S, Kajiwara C, Ishikawa H, Katayama I, Yui K and Udono H: Both CD4+ and CD8+ T cell epitopes fused to heat shock cognate protein 70 (hsc70) can function to eradicate tumors. Cancer Sci 99: 1008-1015, 2008.
27. Shen ZY, Wu MF, Zhang YX, Shen K and Xia GL: Treatment of hepatic carcinoma by low-frequency ultrasound and microbubbles: A case report. Oncol Lett 9: 1249-1253, 2015.
28. Wallace N and Wrenn SP: Ultrasound triggered drug delivery with liposomal nested microbubbles. Ultrasonics 63: 31-38, 2015.
29. Song S, Guo H, Jiang Z, Jin Y, Wu Y, An X, Zhang Z, Sun K and Dou H: Self-assembled microbubbles as contrast agents for ultrasound/magnetic resonance dual-modality imaging. Acta Biomater 24: 266-278, 2015.
30. Lin T, Cai XZ, Shi MM, Ying ZM, Hu B, Zhou CH, Wang W, Shi ZL and Yan SG: In vitro and in vivo evaluation of vancomycin-loaded PMMA cement in combination with ultrasound and microbubbles-mediated ultrasound. Biomed Res Int 2015: 309739, 2015.
31. Kato S, Shirai Y, Kanzaki H, Sakamoto M, Mori S and Kodama T: Delivery of molecules to the lymph node via lymphatic vessels using ultrasound and nano/microbubbles. Ultrasound Med Biol 41: 1411-1421, 2015.
32. Palekar-Shanbhag P, Chogale MM, Jog SV and Gaikwad SS: Microbubbles and their applications in pharmaceutical targeting. Curr Drug Deliv 10: 363-373, 2013.
33. Castle J and Feinstein SB: Ultrasound-directed, site-specific gene delivery. Methods Mol Biol 1141: 67-76, 2014.
34. Byrn SR and Stowell JG: Drug targeting using conjugates: The importance of pharmaceutical chemistry. J Drug Target 3: 239-241, 1995.
35. Jiang J, Xie D, Zhang W, Xiao G and Wen J: Fusion of Hsp70 to Mage-a1 enhances the potency of vaccine-specific immune responses. J Transl Med 11: 300, 2013.
36. Yang FY, Fu WM, Chen WS, Yeh WL and Lin WL: Quantitative evaluation of the use of microbubbles with transcranial focused ultrasound on blood-brain-barrier disruption. Ultrason Sonochem 15: 636-643, 2008.
37. Hernot S and Klibanov AL: Microbubbles in ultrasound-triggered drug and gene delivery. Adv Drug Deliv Rev 60: 1153-1166, 2008.
38. Tung YS, Vlachos F, Feshitan JA, Borden MA and Konofagou EE: The mechanism of interaction between focused ultrasound and microbubbles in blood-brain barrier opening in mice. J Acoust Soc Am 130: 3059-3067, 2011.
39. Bai M, Shen M, Teng Y, Sun Y, Li F, Zhang X, Xu Y, Duan Y and Du L: Enhanced therapeutic effect of Adriamycin on multidrug resistant breast cancer by the ABCG2-siRNA loaded polymeric nanoparticles assisted with ultrasound. Oncotarget 6: 43779-43790, 2015.
40. Wang X, Gkanatsas Y, Palasubramaniam J, Hohmann JD, Chen YC, Lim B, Hagemeyer CE and Peter K: Thrombus-targeted theranostic microbubbles: A new technology towards concurrent rapid ultrasound diagnosis and bleeding-free fibrinolytic treatment of thrombosis. Theranostics 6: 726-738, 2016.